

Quenching of TiO₂ photo catalysis by silver nanoparticles

M. Di Vece^{a,b,*}, A.B. Laursen^a, L. Bech^a, C.N. Maden^a, M. Duchamp^c, R.V. Mateiu^c,
S. Dahl^a, I. Chorkendorff^a

^a Center for Individual Nanoparticle Functionality (CINF), Department of Physics, Technical University of Denmark, DK-2800 Kgs. Lyngby, Denmark

^b Debye Institute for Nanomaterials Science, Nanophotonics—Physics of Devices, Utrecht University, P.O. Box 80000, 3508 TA Utrecht, The Netherlands

^c Center for Electron Nanoscopy (CEN), Technical University of Denmark, DK-2800 Kgs. Lyngby, Denmark

ARTICLE INFO

Article history:

Received 16 September 2011

Received in revised form

20 December 2011

Accepted 21 December 2011

Available online 11 January 2012

Keywords:

Plasmonics

Photo-catalysis

Ethylene

Oxidation

Thin films

Nanoparticle

ABSTRACT

The plasmon resonance of metal nanostructures affects neighboring semiconductors, quenching or enhancing optical transitions depending on various parameters. These plasmonic properties are currently investigated with respect to topics such as photovoltaics and optical detection and could also have important consequences for photocatalysis. Here the effect of silver nanoparticles of a size up to 30 nm and at maximum 0.50 monolayers on the photocatalytic oxidation of ethylene on TiO₂ is studied. Since the plasmon resonance energy of silver nanoparticles is comparable with the TiO₂ band gap, dipole–dipole interaction converts excitons into heat at the silver nanoparticle. This indicates that plasmonic interaction with TiO₂ semiconductor catalysts can reduce the photo catalytic activity considerably.

© 2012 Elsevier B.V. All rights reserved.

1. Introduction

The interaction of light with metal nanostructures is the research subject of plasmonics and merges electronics with optics [1,2] at small scales. A plasmon is the collective oscillation of an electron gas. This oscillation can be set in motion by an external electromagnetic field, which in turn can generate radiation. This complex response opens a wide range of possible studies and applications, not in the least due to the much smaller spatial dimensions of this phenomenon as compared to traditional optical components [3]. In photovoltaics the implementation of such plasmonic nanostructures is currently explored with respect to wave guiding and increased scattering [4]. One of the currently investigated properties is the so-called plasmonic field enhancement. The excitation of plasmon modes by an incident electromagnetic wave can enhance the pump rate of a nearby emitter due to local field enhancement. The electromagnetic field close to the metal surface is enhanced by orders of magnitude and used to strongly excite luminescent dyes in the vicinity of metallic nanostructures [3].

* Corresponding author at: Debye Institute for Nanomaterials Science, Nanophotonics—Physics of Devices, Utrecht University, P.O. Box 80000, 3508 TA Utrecht, The Netherlands. Tel.: +31 30 253 4190; fax: +31 30 254 3165.

E-mail address: m.divece@uu.nl (M. Di Vece).

The coupling of an emitter to plasmon modes affects both the radiative and non-radiative decay rates. This phenomenon is based on the principle that the strength with which an emitter couples with an electromagnetic field depends on its environment [5]. A metal particle with a plasmon resonance frequency that matches the emission frequency of an emitter will modify the electric fields in such a way that the electromagnetic field generated by the emitter is enhanced. Analogous to the energy being captured from the incident electromagnetic wave, also the energy from the emitter can be transferred to plasmon modes of a nanoparticle. This energy will partially be dissipated and partially be coupled to radiation.

The balance between dissipation and radiation depends strongly on the geometry. Despite the presence of dissipation due to Ohmic losses, the luminescence intensity of an optical emitter can be enhanced by several orders of magnitude [6]. Early work in conjunction with surface enhanced Raman spectroscopy, SERS, showed such photoluminescence enhancements with rough metal surfaces [7,8]. Recent studies showed that the photoluminescence enhancement and quenching depends on the distance between emitter and metal [9], with concomitant changes in excited lifetime [10–12].

The effect of plasmonics in photocatalysis is subject of recently started research with the considerations of Nitzan and Brus [13] and the soon following results on photodissociation of dimethyl cadmium [14]. A recent study about methylene decomposition under the influence of local field enhancement by silver nanoparticles shows a significant increase of activity [15]. In this work we

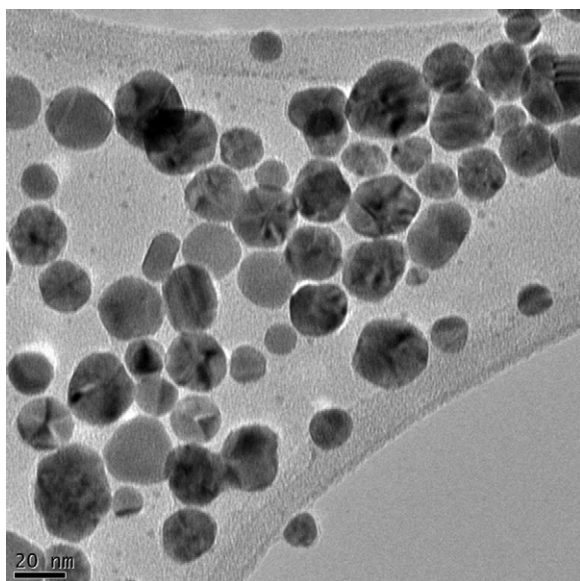


Fig. 1. TEM micrograph of silver nanoparticles as deposited on a holey carbon grid from solution. The scale bar is 20 nm.

investigate the plasmonic effect of silver nanoparticles on the catalytic activity of TiO_2 . TiO_2 is the most widely used photocatalyst employed for the oxidation of organic chemicals [16,17]. TiO_2 exists in three different crystalline forms: rutile, anatase and brookite, with anatase having shown most photocatalytic activity. Since the band gap energy of TiO_2 and the silver plasmon resonance energy are close together an interaction is expected. Whether the radiative and non-radiative decay are inhibited or photo absorbance enhanced needs to be established. Both possibilities are contributing to increased photocatalytic activity. In case the opposite effects are present, the photocatalytic activity will be quenched. This has important consequences from an application point of view. Due to its simplicity ethylene photo oxidation on TiO_2 forms a good model system and produces only CO_2 and H_2O [18,19]. Furthermore, ethylene is a common molecule, both used in the chemical industry and abundant in nature as for example a fruit-ripening hormone [20], and hence its gas phase removal is also of industrial interest [21,22].

2. Materials and methods

The TiO_2 layer was deposited on Pyrex wafers by spin coating a commercial aqueous solution containing TiO particles (Ebonik DEGUSSA VpDisp W2730 30 wt.% TiO_2 without additives) at 2000 rpm for 3 s. XRD on the TiO_2 showed a constitution of 84% anatase and 16% rutile. The Pyrex wafers are circular with a diameter of 10 cm. The deposited TiO_2 was annealed at 400°C for 1 h, which dehydrates the film.

The silver colloids were synthesized from AgNO_3 . Ethylene glycol was used as solvent and reducing agent for AgNO_3 . Polyvinylpyrrolidone (Sigma–Aldrich PVP K15, Mw 10,000) was used as a protecting agent. The synthesis follows the procedure reported in literature [23]. All chemicals were of reagent purity. The Ag colloids are washed by centrifugation at 10,000 rpm for 30 min 3 times in acetone and subsequently dispersed in ethanol by sonication for 10 min. This solution (4.2 mM silver) is then spin coated onto the TiO_2 layer (2000 rpm, 3 s), note that the colloids were sonicated 5–10 min immediately before applying, to disperse any agglomerates. In Fig. 1 the Ag colloids are shown by TEM, they have a broad size range of up to about 30 nm. The total amount of silver nanoparticles can be estimated from the silver absorbance coefficient [24] and the here measured optical absorbance. For the low,

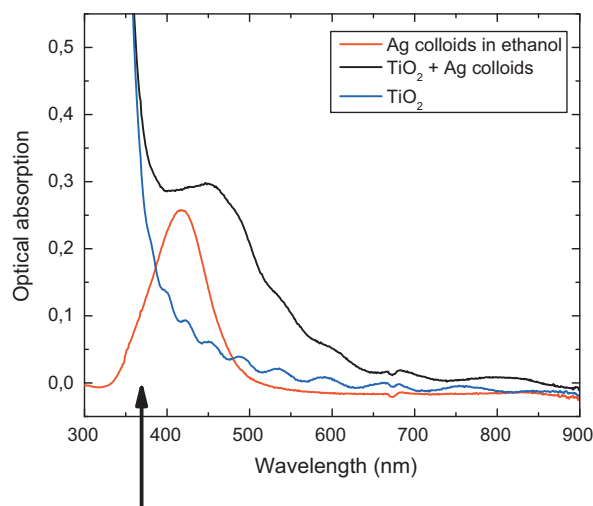


Fig. 2. Optical absorbance spectrograms of pure TiO_2 (blue), silver nanoparticles in ethanol (red) and silver nanoparticles in TiO_2 (black). The arrow indicates the illumination wavelength during the photocatalysis experiment. (For interpretation of the references to color in this figure legend, the reader is referred to the web version of the article.)

medium and high silver nanoparticle concentration, an equivalent of 0.14, 0.22 and 0.55 monolayer's silver nanoparticles is estimated.

Gas Chromatography was performed with a Totalchrom (PerkinElmer) with a constant flow of 125 ml/min in the 406 ml total volume in a recirculation loop with the reactor cell. Before every experiment the system was flushed with synthetic air until only oxygen and nitrogen are observed (20 min). Several minutes after ethylene gas was manually injected in the cell, the UV lamp was turned on. The TiO_2 layers are irradiated with UV light at 365 nm with a 4 watt, UVGL-15 compact UV lamp. The experiments were performed at room temperature and the temperature inside the reactor during UV irradiation remained constant.

Transmission electron microscopy and scanning electron microscopy were performed with a TECNAI T20 microscope and a QUANTA 200 FEG MKII microscope, respectively. X-ray photoelectron spectroscopy (XPS) was done with monochromatized Al $K\alpha$ radiation and energy resolution corresponding to 1.0 eV FWHM of Ag $3d_{5/2}$, using a Theta Probe set-up from Thermo Fisher Scientific. Charge compensation during XPS was accomplished by flooding with electrons and argon ions. No sample damage could be observed during XPS measurements. The binding energy 458.6 eV for Ti $2p_{3/2}$ of TiO_2 is used as reference.

X-ray fluorescent spectroscopy was used for elemental quantification. An internal standard of $\text{Mn}(\text{CHOO})_2$ together with AgNO_3 in 1:1 EtOH/ H_2O was used to quantify Ag colloids concentrations. The washed solution was determined to be 61.8 mM in concentration.

3. Results and discussion

The TiO_2 layer with and without silver colloids are investigated by measuring the optical absorbance spectra as shown in Fig. 2. A distinct plasmon peak is observed in the optical absorbance of the silver colloids dissolved in ethanol in good agreement with literature. The narrow width of the plasmon resonance peak indicates small size dispersion. The optical absorbance spectrum of the TiO_2 layer provides the band gap energy at 3.1 eV (360 nm). After deposition of the silver colloids the silver plasmon peak has been red shifted by about 50 nm from 410 to 460 nm due to a different dielectric environment since the ethanol has been evaporated and the silver colloids are likely transported by capillary forces inside the porous TiO_2 film. XPS measurements (which is surface sensitive)

show a Ag:Ti ratio of about 0.08 on the surface for the medium concentration, indicating a low silver content as compared to titanium. If the surface would consist of only silver nanoparticles a close to 100% Ag content would have been measured. This confirms that only a fraction of the silver nanoparticles remains on the surface. The total amount of silver nanoparticles within the entire TiO₂ film can be estimated from the silver absorbance coefficient [24] of a known concentration of silver nanoparticles on TiO₂ and the here measured optical absorbance at the silver plasmon frequency. For the low, medium and high silver nanoparticle concentration, an equivalent of 0.14, 0.22 and 0.50 monolayer's silver nanoparticles is estimated.

In Fig. 3a SEM micrograph of the TiO₂ film is shown, the cross section provides a good estimate of the thickness, which in this case is about 1.5 μm. The contrast differences on the 10–50 nm scale indicate a large porosity; the white specs are likely individual TiO₂ particles. With an optical absorbance at 365 nm in the TiO₂ film of 0.41, (the absorbance coefficient can be estimated to $3.4 \times 10^4 \text{ cm}^{-1}$) the entire film receives enough energy to excite valence band electrons to the conduction band.

The photocatalytic activity was monitored by measuring the ethylene concentration as a function of time as provided by the flame ionization detector (FID) of the gas chromatograph. In order to obtain a good time resolution, 200 μL ethylene (AGA, 99.95% purity) was injected before the start of each measurement, resulting in full oxidation after about 2.5 h. No catalytic activity was observed without illumination while the start of the experiment was set by turning on the lamp. In Fig. 4 the ethylene concentration transients are shown for only the TiO₂ layer and three experiments with increasing silver particle concentration. The TiO₂ layer without silver nanoparticles needs about 140 min to completely oxidize ethylene while the TiO₂ layers with silver nanoparticles need about 200 min. Remarkably, the concentration of silver nanoparticles does not affect the oxidation time indicating that a threshold silver nanoparticle concentration results in a similar reduced oxidation time. After prolonged illumination the sample became slightly grayish, indicating some oxidation of the silver nanoparticles, this seems not to influence the quenching effect. The concentration versus time curve of the TiO₂ layer without silver nanoparticles is curved and could be well fitted with an exponential decay function, suggesting that the ethylene concentration is the rate determining factor. Instead, the concentration transients of the TiO₂ with silver nanoparticles are linear, which is a sign that the oxidation rate is independent of the ethylene concentration; a constant amount of ethylene is oxidized per time interval. The latter is possible if fewer oxidation sites are available due to the presence of silver nanoparticles.

Since the silver nanoparticle concentration is low, it is unlikely that the silver nanoparticles significantly block ethylene diffusion within the TiO₂ layer. Considering the low concentration, screening of TiO₂ is negligible. The silver nanoparticles can act as ethylene oxidation catalyst, which in this case does not have a strong effect due to the low temperature [25,26]. A control measurement with only the solvent (ethanol) deposited on the TiO₂ layer had a comparable oxidation time as the TiO₂ layer without silver nanoparticles. To investigate whether traces of PVP used in the production of the silver nanoparticles could be present on the TiO₂ layer, affecting the overall ethylene oxidation time, the surface composition before and after deposition of the silver nanoparticles was analysed using XPS as shown in Fig. 5. PVP contains a nitrogen atom and a carbonyl group for each unit. After deposition, XPS gives a nitrogen content below 0.3%, corresponding to less than a fifth of the silver concentration. A small amount of nitrogen was also present before the deposition, so it is not obvious whether there is a small extra contribution from remnants of PVP. The absence of carbonyl present in pristine PVP is clearly demonstrated by the fine structure of the

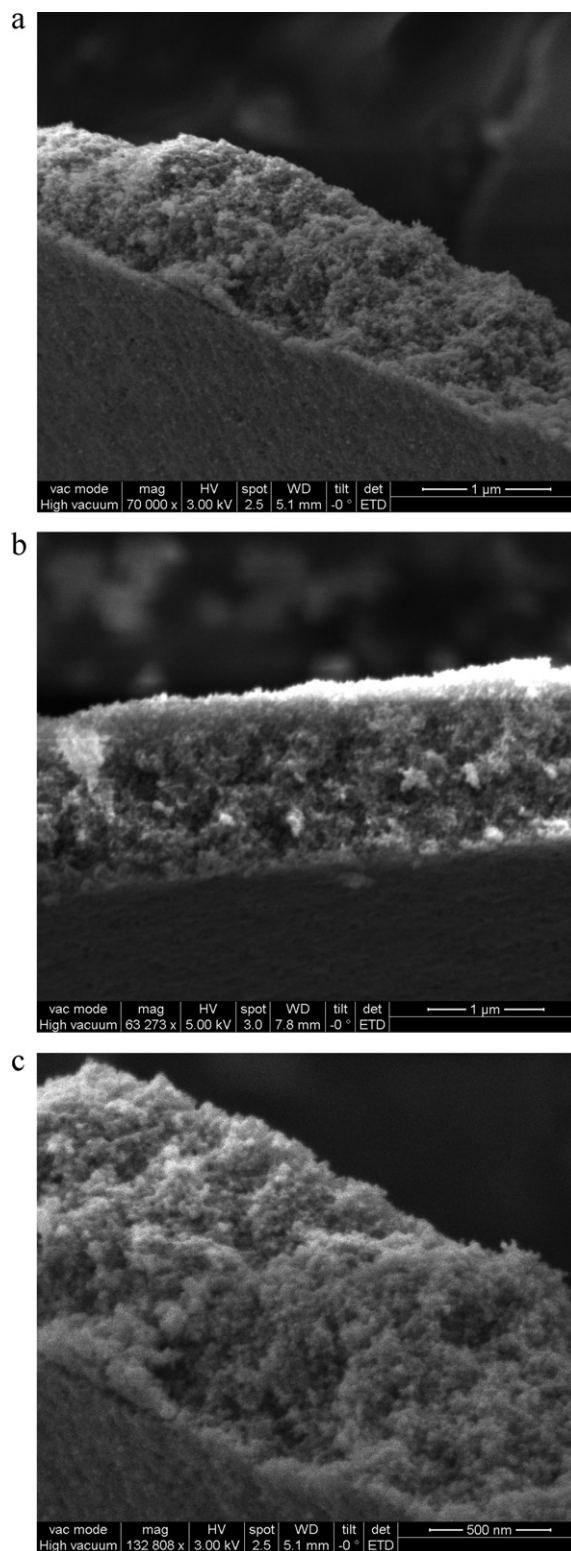


Fig. 3. SEM micrograph of a: (a) TiO₂ layer with silver nanoparticles (not distinguishable), (b) TiO₂ layer without silver nanoparticles and (c) close up of TiO₂ layer illustrating high porosity.

C 1s spectrum. In PVP, the carbonyl group component is shifted 2.8 eV relative to sp²-hybridized carbon [27] unaffected by silver nanoparticle capping [28,29]. sp²-hybridized carbon is a main constituent in PVP, but occurs also as a common contaminant species. It is attributed to the dominant C 1s feature observed at 284.6 eV (referenced to Ti 2p_{3/2} at 458.6 eV). The absence of PVP carbonyl

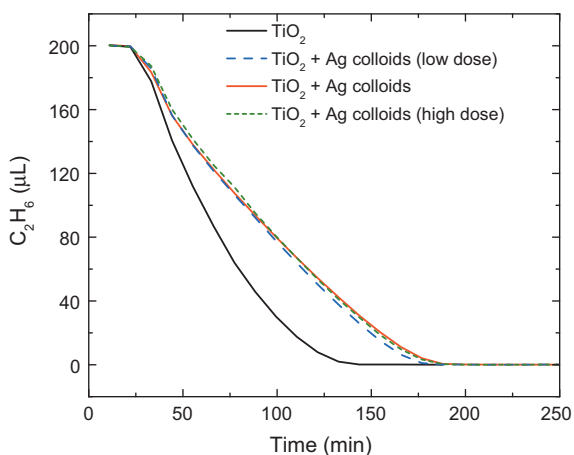


Fig. 4. Ethylene concentration transients (normalized) during illumination of TiO₂ at 365 nm with a pure TiO₂ layer (black), a TiO₂ layer and silver colloids at low (dashed blue), medium (red) and high (dotted green) dose 200 μL of ethylene was injected before the start of each measurement. (For interpretation of the references to color in this figure legend, the reader is referred to the web version of the article.)

groups is evident from the clear separation between the two other C 1s components, which are observed at 1.5 and 4.2 eV higher binding energy, respectively. Furthermore, the binding energies of the C 1s components observed before and after deposition are similar, suggesting that the type of carbon contamination did not change. This demonstrates that a PVP contamination cannot be the cause of the reduced ethylene oxidation time.

The formation of a Schottky barrier at the silver–TiO₂ nanoparticle interface could cause a charge carrier separation leading to charging of the TiO₂ and Ag nanoparticles. Considering the very low amount of silver nanoparticles this mechanism unlikely reduces the catalytic performance of TiO₂ by the inclusion of silver nanoparticles.

An explanation of the reduced oxidation capability of TiO₂ with silver nanoparticles therefore lays likely in the plasmonic interaction of the silver nanoparticles with the photo-excited electron–hole pairs. The photoluminescence quenching by gold nanoparticles on luminescent dyes demonstrates that the energy of

excitons can be transferred to a metal nanoparticle and transformed into heat [12]. This mechanism is probably the cause of the reduced oxidation in the TiO₂ layer with silver nanoparticles. The plasmon resonance wavelength of the silver particles within the TiO₂ film occurs at about 450 nm which is 2.7 eV. Excitons in TiO₂ with that energy or higher will be scavenged by the silver nanoparticles and transformed into heat. Excitons with lower energy remain available in TiO₂ for ethylene oxidation. If the plasmon resonance energy would be higher than the TiO₂ band gap, quenching will not be possible as transfer of energy will not be allowed. The exciton lifetime in TiO₂ is of the order of a few nanoseconds [30], which provides enough time to travel towards the vicinity of silver nanoparticles.

Some excitons in TiO₂ can be bound, self-trapped on TiO₆ octahedra [31], they probably do not contribute to the photocatalytic process. In many studies metal nanoparticles of platinum or gold are added to photocatalysts such as TiO₂ which enhance the overall activity [32,18]. However, these nanoparticles are often too small to have a significant plasmon resonance; hence they most likely work as co-catalysts. Whether the presence of metal nanoparticles results in enhancement or quenching strongly depends on the distance between the metal and semiconductor [9]. For example, the oxidation of methylene was significantly enhanced by the presence of silver nanoparticles which were positioned at a distance of approximately 20 nm by a SiO₂ layer [15]. In contrast, this work shows that when the silver particles are in close contact with the semiconductor, quenching dominates.

4. Conclusions

The presence of silver nanoparticles in TiO₂ porous layers, have an adverse effect on the photocatalytic oxidation of ethylene. Excitons with an energy which is comparable to the silver nanoparticle plasmon energy are scavenged by dipole–dipole interaction and transformed into heat. This work demonstrates that the combination of semiconductors and metal nanoparticles for photocatalysis can inhibit the performance. Different geometries or off-resonance between the semiconductor band gap and metal nanoparticle plasmon energy are needed to further study the plasmonic effect on photocatalysts.

Acknowledgements

CINF is funded by the Danish National Research Foundation, and this project was supported by the Danish Technology Foundation.

References

- [1] E. Ozbay, Science 311 (2006) 189–193.
- [2] S.A. Maier, M.L. Brongersma, P.G. Kik, S. Meltzer, A.A.G. Requicha, H.A. Atwater, Adv. Mater. 13 (2001) 150–155.
- [3] J.A. Schuller, E.S. Barnard, W. Cai, Y.C. Jun, J.S. White, M.L. Brongersma, Nat. Mater. 9 (2010) 193–204.
- [4] H.A. Atwater, A. Polman, Nat. Mater. 9 (2010) 205–213.
- [5] E. Purcell, Phys. Rev. 69 (1946) 68–681.
- [6] J.S. Biteen, D. Pacifici, N.S. Lewis, H.A. Atwater, Nano Lett. 5 (2005) 1768–1773.
- [7] M. Moskovits, Rev. Mod. Phys. 57 (1985) 783–826.
- [8] A. Wokaun, H.-P. Lutz, A. King, U. Wild, R. Ernst, J. Chem. Phys. 79 (1983) 509–511.
- [9] P. Anger, P. Bharadwaj, L. Novotny, Phys. Rev. Lett. 96 (2006) 113002.
- [10] J.N. Farahani, D.W. Pohl, H.-J. Eisler, B. Hecht, Phys. Rev. Lett. 95 (2005) 017402.
- [11] S. Kuhn, U. Hakanson, L. Logobete, V. Sandoghar, Phys. Rev. Lett. 97 (2006) 017402.
- [12] T. Pons, I.L. Medintz, K.E. Sapsford, S. Higashiya, A.F. Grimes, D.S. English, H. Mattoussi, Nano Lett. 7 (2007) 3157–3164.
- [13] A. Nitzan, L.E. Brus, J. Chem. Phys. 75 (1981) 2205–2214.
- [14] C.J. Chen, R.M. Osgood, Phys. Rev. Lett. 50 (1983) 1705–1708.
- [15] K. Awazu, et al., J. Am. Chem. Soc. 130 (2008) 1676–1680.
- [16] O. Carp, C.L. Huisman, A. Reller, Progr. Sol. Stat. Chem. 32 (2004) 33–177.
- [17] J. Wilcoxon, B.L. Abrams, Nanotechnology 2 (2008) 51–124.
- [18] M. Zorn, De Tompkins, W. Zeltner, M. Anderson, Environ. Sci. Technol. 34 (2000) 5206–5210.

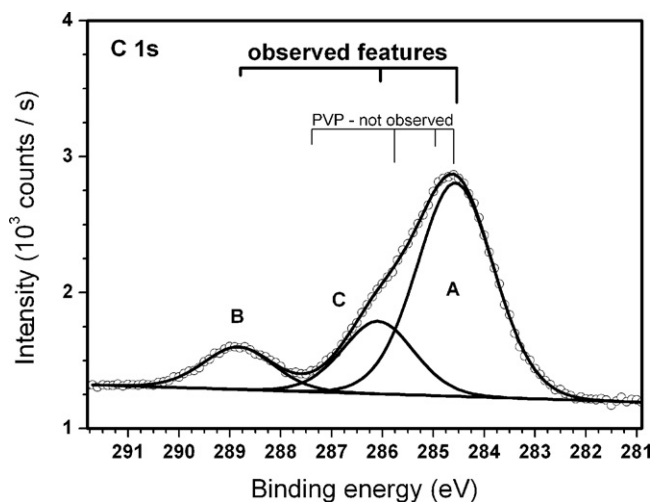


Fig. 5. XPS spectrum of C 1s, deconvoluted into three components A, B and C. The dominant feature A appears at 284.6 eV in good agreement with the expectations for hydrocarbons. The thin bars indicate the chemical shifts expected for PVP [27]. The absence of the PVP carbonyl groups is evident from the clear separation between the two other C 1s components B and C, which are observed at 1.5 and 4.2 eV higher binding energy, respectively.

- [19] S. Yamazaki, S. Tanaka, H. Tsukamoto, *J. Photochem. Photobiol. A: Chem.* 121 (1999) 55–56.
- [20] S.P. Burg, E.A. Burg, *Science* 148 (1965) 1190–1196.
- [21] S. Qida, *Vacuum* 44 (2007) 63–66.
- [22] C. Maneerat, Y. Hayata, N. Egashira, K. Sakamoto, Z. Hamai, M. Kuroyanagi, *Trans. ASAE* 46 (2003) 725–730.
- [23] P.-Y. Silvert, R. Herrera-Urbina, N. Duvauchelle, V. Vijayakrishnan, K.T. Elhsissen, *J. Mater. Chem.* 6 (4) (1996) 573–577.
- [24] L.G. Schultz, *J. Opt. Soc. Am.* 44 (1954) 357.
- [25] A. Nagy, Gerhard Mestl, *Appl. Catal. A: Gen.* 188 (1999) 337–353.
- [26] Y. Shiraiishi, N. Toshima, *Colloids Surf. A: Physicochem. Eng. Aspects* 169 (2000) 59–66.
- [27] K. Chan, L.E. Kostun, W.E. Tenhaeff, K.K. Gleason, *Polymer* 47 (2006) 6941–6947.
- [28] Y. Wang, Y. Li, S. Yang, G. Zhang, D. An, C. Wang, Q. Yang, X. Chen, X. Jing, Y. Wei, *Nanotechnology* 17 (2006) 3304–3307.
- [29] T. Zhao, R. Sun, S. Yu, Z. Zhang, L. Zhou, H. Huang, R. Du, *Colloids Surf. A: Physicochem. Eng. Aspects* 366 (2010) 197–202.
- [30] K. Fujihara, S. Izumi, T. Ohno, M. Matsumura, *J. Photochem. Photobiol. A: Chem.* 132 (2000) 99–104.
- [31] H. Tang, H. Berger, P.E. Schmid, F. Levy, G. Burri, *Sol. Stat. Commun.* 87 (1993) 847–850.
- [32] A.V. Vorontsov, I.V. Stoyanova, D.V. Kozlov, V.I. Simagina, E.N. Savinov, *J. Catal.* 189 (2000) 360–369.